Magnetic order and crystal-field excitations in $Nd_3Pd_{20}Ge_6$

1998 J. Phys.: Condens. Matter 10 7219

(http://iopscience.iop.org/0953-8984/10/32/013)

J. Phys.: Condens. Matter **10** (1998) 7219–7229. Printed in the UK PII: S0953-8984(98)93058-2

Magnetic order and crystal-field excitations in $Nd_3Pd_{20}Ge_6$

A Dönni†+, L Keller‡, P Fischer‡, Y Aoki§, H Sato§, F Fauth‡*, M Zolliker‡*, T Komatsubara‖ and Y Endoh¶

† Department of Physics, Niigata University, Niigata 950-2181, Japan
‡ Laboratory for Neutron Scattering, ETH Zürich and Paul Scherrer Institute, CH-5232 Villigen PSI, Switzerland
§ Department of Physics, Faculty of Science, Tokyo Metropolitan University, Hachioji-shi 192-03, Japan
‖ Centre for Low Temperature Science, Tohoku University, Sendai 980-8578, Japan
¶ Department of Physics, Graduate School of Science, Tohoku University, Sendai 980-8578, Japan

Received 1 April 1998, in final form 26 May 1998

Abstract. The magnetic properties of the new cubic intermetallic compound $Nd_3Pd_{20}Ge_6$ have been investigated by neutron scattering and low-temperature specific heat experiments. The results include the refinement of the crystal structure at 10 K (space group $Fm\bar{3}m$, No 225), the observation of three successive magnetic phase transitions (at $T_{N1} = 1.75$ K, $T_{N2} = 1.40$ K and $T_{N3} = 0.54$ K), the determination of the antiferromagnetic structure between T_{N1} and T_{N2} (antiferromagnetically ordered Nd moments on site 8c coexist with disordered Nd moments on site 4a) and the measurement of the crystalline-electric-field (CEF) level scheme ($\Gamma_8^{(1)} \rightarrow \Gamma_6 \rightarrow \Gamma_8^{(2)}$) in the paramagnetic state. An extrapolation of the CEF parameters obtained for $Nd_3Pd_{20}Ge_6$ predicts the CEF ground-states to be the triplet Γ_5 in $Pr_3Pd_{20}Ge_6$ and the quartet Γ_8 in $Ce_3Pd_{20}Ge_6$.

1. Introduction

Recently the ternary intermetallic Kondo compound $Ce_3Pd_{20}Ge_6$ has attracted interest because quadrupolar ordering at $T_Q \approx 1.2$ K occurs at higher temperature than antiferromagnetic ordering at $T_N \approx 0.75$ K [1]. The cubic crystal structure of $Ce_3Pd_{20}Ge_6$ (space group $Fm\bar{3}m$, No 225, $Z = 4$, with the sites 4a and 8c occupied by Ce, 32f and 48h by Pd and 24e by Ge atoms) is an ordered derivative of the $Cr_{23}C_6$-type structure [2] and magnetic Ce atoms occupy two different crystallographic sites both with cubic point symmetry. Experimental evidence for the quadrupolar phase transition at $T_Q \approx 1.2$ K are (a) a small rounded specific heat anomaly [1]; (b) a maximum in the electrical resistivity [1]; (c) a well defined minimum of the elastic constant $(C_{11} - C_{12})/2$ measured by ultrasonics [3] and (d) the absence of magnetic neutron Bragg intensity above T_N [4]. Crystalline-electric-field (CEF) interactions of cubic symmetry split the sixfold degenerate J-multiplet $2F_{5/2}$ of Ce^{3+} in $Ce_3Pd_{20}Ge_6$ into a quartet (Γ_8) and a doublet (Γ_7). The

+ Author for further correspondence: Andreas Dönni, Department of Physics, Niigata University, Ikarashi 2-8050, Niigata 950-2181, Japan. E-mail address: donni@sc.niigata-u.ac.jp.
* Present address: Institute Laue–Langevin (ILL), F-38042 Grenoble, France.

0953-8984/98/327219+11$19.50

magnetic entropy [1] reveals that certainly for the site 8c and probably also for the site 4a the CEF ground-state is the quartet Γ_8, which possesses an electronic quadrupolar moment as well as a magnetic dipole moment. The magnetic phase diagram of $Ce_3Pd_{20}Ge_6$ determined from single crystal specific heat data suggests the existence of a complicated form of anisotropic interaction between electric quadrupolar moment and the magnetic dipolar moment [5].

These interesting results on $Ce_3Pd_{20}Ge_6$ have motivated us to extend the investigation to the new Kramers doublet system $Nd_3Pd_{20}Ge_6$ which was confirmed to be isostructural to $Ce_3Pd_{20}Ge_6$. In this paper we present an overview of the magnetic properties measured on a polycrystalline $Nd_3Pd_{20}Ge_6$ sample by low-temperature specific heat (down to 0.12 K), neutron diffraction (down to 1.45 K) and inelastic neutron scattering (above 5 K). The results include the refinement of the crystal structure at 10 K (section 3.1), the observation of three successive magnetic phase transitions between 0.54 and 1.75 K (section 3.2), the determination of the magnetic structure down to 1.45 K (section 3.2) and the measurement of the CEF level scheme in the paramagnetic state (section 3.3).

2. Experiment

Polycrystalline $Nd_3Pd_{20}Ge_6$ samples were synthesized by arc-melting stoichiometric mixtures of the pure elements in an argon atmosphere and were annealed in an evacuated quartz tube for 7 days at 800 °C. In order to search for magnetic phase transitions in $Nd_3Pd_{20}Ge_6$ low temperature specific heat experiments between 0.12 and 7 K were carried out at the Tokyo Metropolitan University using a semiadiabatic heat-pulse method.

Neutron scattering experiments on $Nd_3Pd_{20}Ge_6$ were performed partly at the high-flux reactor of the Institute Laue–Langevin (ILL) in Grenoble, France, on the powder diffractometer D1A and on the triple-axis spectrometer IN3 and partly at the new neutron spallation source SINQ at the Paul Scherrer Institute (PSI) in Villigen, Switzerland, on the powder diffractometer DMC. A large amount (18 g) of fine $Nd_3Pd_{20}Ge_6$ powder was filled under helium gas atmosphere into cylindrical vanadium containers (D1A and DMC) or aluminum containers (IN3) and mounted in a standard ^{4}He Orange cryostat. Crystal and magnetic structures of $Nd_3Pd_{20}Ge_6$ were studied at 1.45 and 10 K on D1A with a neutron wavelength $\lambda = 2.483$ Å (obtained from a vertically focused germanium (0, 0, 4) monochromator) and between 1.6 and 3.0 K on DMC with $\lambda = 4.209$ Å (obtained from a vertically focussed graphite (0, 0, 2) monochromator). On D1A a pyrolitic graphite filter was placed between monochromator and sample in order to reduce higher-order contamination, while on DMC a beryllium filter was used for the same reason. The diffraction patterns were analysed by the Rietveld method with the program FullProf [6] using the neutron scattering lengths published by Sears [7] and the relativistic magnetic form factors of Nd^{3+} in dipolar approximation. The background was described with a five-order polynomial and peak-shape with a pseudo-Voigt function.

CEF excitations of $Nd_3Pd_{20}Ge_6$ were measured in the paramagnetic state between 5 and 100 K on IN3 for energy transfers up to 20 meV. In order to gain intensity a horizontally and vertically focusing monochromator (copper (1, 1, 1)) and a horizontally focusing analyser (graphite (0, 0, 2)) were used. Constant-$\boldsymbol{Q}$ scans were performed for moduli of the scattering vector $\boldsymbol{Q}$ of 1.60 Å^{-1} and 3.80 Å^{-1} with the energy of the scattered neutrons E_f fixed at 13.7 meV. In order to reduce higher-order contamination a pyrolitic graphite filter was placed in the scattered neutron beam. The energy resolution at the elastic peak ($\Delta E = 0$) turned out to be $\delta E = 0.47$ meV (full width at half maximum).

3. Results and discussion

3.1. The crystal structure

The D1A powder neutron diffraction pattern of $Nd_3Pd_{20}Ge_6$ in its paramagnetic state at 10 K is shown in figure 1. The observed intensity distribution confirms that $Nd_3Pd_{20}Ge_6$ is isostructural to $Ce_3Pd_{20}Ge_6$ (cubic space group $Fm\bar{3}m$, No 225, with the sites 4a and 8c occupied by Nd, 32f and 48h by Pd and 24e by Ge atoms). A FullProf refinement in the scattering angle range $15^\circ < 2\Theta < 150^\circ$ of 32 inequivalent nuclear Bragg reflections (with different 2Θ values) yielded the structural parameters given in table 1. The agreement

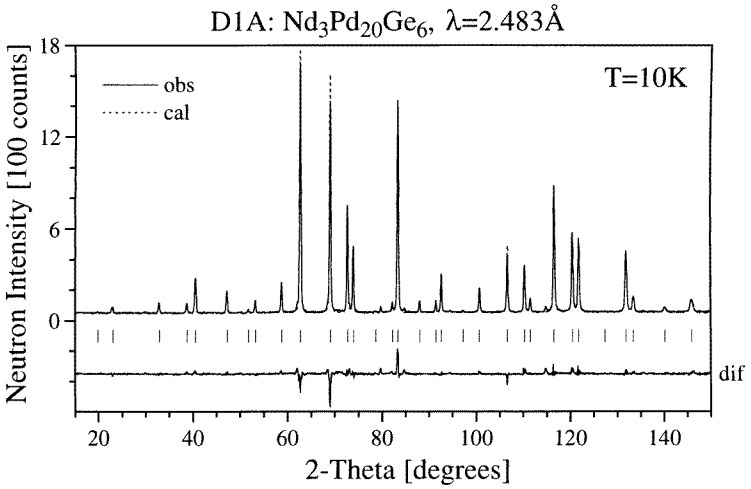

Figure 1. Observed, calculated and difference D1A neutron diffraction patterns ($\lambda = 2.483$ Å) of paramagnetic $Nd_3Pd_{20}Ge_6$ at 10 K. Peak positions are indicated by vertical bars.

Table 1. Parameters of crystal structure and selected interatomic distances of paramagnetic $Nd_3Pd_{20}Ge_6$ at 10 K refined from D1A powder neutron diffraction data. The Debye–Waller factor was kept fixed for all atoms at $B = 0.1$ Å^2.

$Fm\bar{3}m$ (No 225)		$a = 12.383(5)$ Å			
Atom	Site	x/a	y/a	z/a	$Z = 4$
Nd1	4a	0	0	0	
Nd2	8c	1/4	1/4	1/4	
Pd1	32f	x	x	x	$x = 0.3836(2)$
Pd2	48h	0	y	y	$y = 0.1752(2)$
Ge1	24e	x	0	0	$x = 0.2680(2)$
Nd1–Pd2	(12×)	3.068(5) Å			
–Ge1	(6×)	3.319(4) Å			
–Nd2	(8×)	5.362(2) Å			
–Nd1	(6×)	8.756(4) Å			
Nd2–Pd1	(4×)	2.865(1) Å			
–Pd2	(12×)	3.361(3) Å			
–Nd1	(4×)	5.362(2) Å			
–Nd2	(6×)	6.192(3) Å			

values of the FullProf fit were $R_{wp} = 7.53\%$ and $R_{I,N} = 6.14\%$, concerning weighted and integrated intensities, respectively. From counting statistics, the expected value was $R_{exp} = 3.99\%$, yielding $\chi^2 = (R_{wp}/R_{exp})^2 = 3.57$. Traces of an unidentified impurity phase in the D1A pattern (e.g., see weak peaks at $2\Theta = 79.65^\circ$ and at 114.70° in figure 1) were neglected in the refinement.

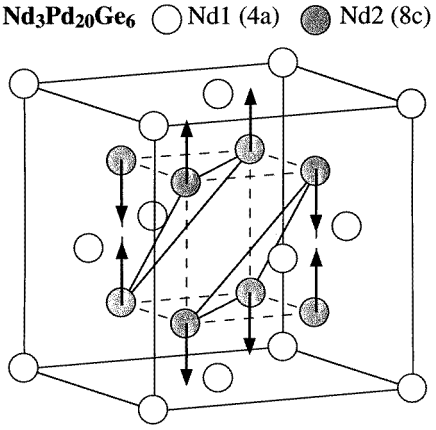

Figure 2. The arrangement of magnetic Nd atoms (on sites 4a and 8c) in the crystallographic unit cell of $Nd_3Pd_{20}Ge_6$. Arrows indicate the antiferromagnetic coupling of the ordered Nd2 moments between T_{N2} and T_{N1}. Note that because the configurational symmetry is cubic it is impossible to determine the direction of the ordered Nd2 moments (plotted along the [0, 0, 1] direction, as favoured by the small crystal-electric-field anisotropy) in a zero-field neutron diffraction experiment.

The crystallographic unit cell of $Nd_3Pd_{20}Ge_6$ with a volume of 1898(2) $Å^3$ is quite large and contains 116 atoms. The arrangement of the magnetic Nd atoms on two different sites is illustrated in figure 2. Nd1 atoms on site 4a form a face-centred cubic lattice with a 'larger' lattice parameter a, whereas Nd2 atoms on site 8c form a simple cubic lattice with a 'smaller' lattice parameter $a/2$. Interatomic Nd–Nd distances at 10 K are shortest for Nd1–Nd2 (5.362(2) Å), followed by Nd2–Nd2 (6.192(3) Å) and Nd1–Nd1 (8.756(4) Å). The coordination polyhedra for Nd1 and Nd2 are shown in figure 3. Nd1 atoms have 12 nearest neighbours (Pd2 at 3.068(5) Å) and six second-nearest neighbours (Ge1 at 3.319(4) Å), whereas Nd2 atoms are surrounded by 16 Pd atoms (four Pd1 at 2.865(1) Å and 12 Pd2 at 3.361(3) Å).

The symmetry of the face-centred cubic crystal structure of $Nd_3Pd_{20}Ge_6$ allows Bragg peaks with only odd indices (e.g., (1, 1, 1), (3, 1, 1), (3, 3, 1), ...) and those with only even indices (e.g., (2, 0, 0), (2, 2, 0), (2, 2, 2), ...). Reflecting the different extinction rules of the sites 4a and 8c, the Nd1 atoms contribute to all nuclear Bragg peaks, whereas the Nd2 atoms to only those with even indices. This fact proves to be helpful to distinguish contributions to the magnetic structures arising from the Nd1 and the Nd2 atoms.

3.2. Magnetic phase transitions

The temperature variation of the specific heat per formula unit $Nd_3Pd_{20}Ge_6$ is displayed in figure 4. Specific heat anomalies indicate three successive magnetic phase transitions at $T_{N1} = 1.75$ K, $T_{N2} = 1.40$ K and $T_{N3} = 0.54$ K and at lowest temperature the additional increase of C_p from 0.15 K towards 0.12 K might be due to the nuclear contribution of Nd

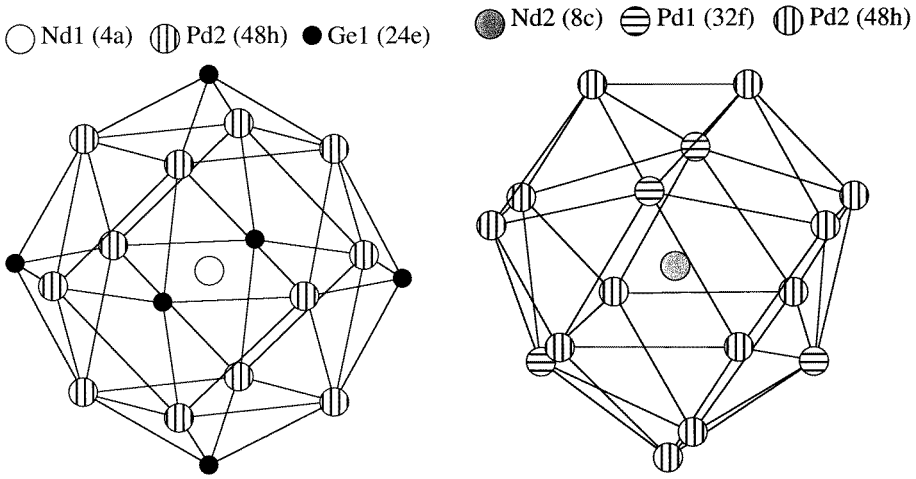

Figure 3. Coordination polyhedra for Nd1 on site 4a and for Nd2 on site 8c in $Nd_3Pd_{20}Ge_6$.

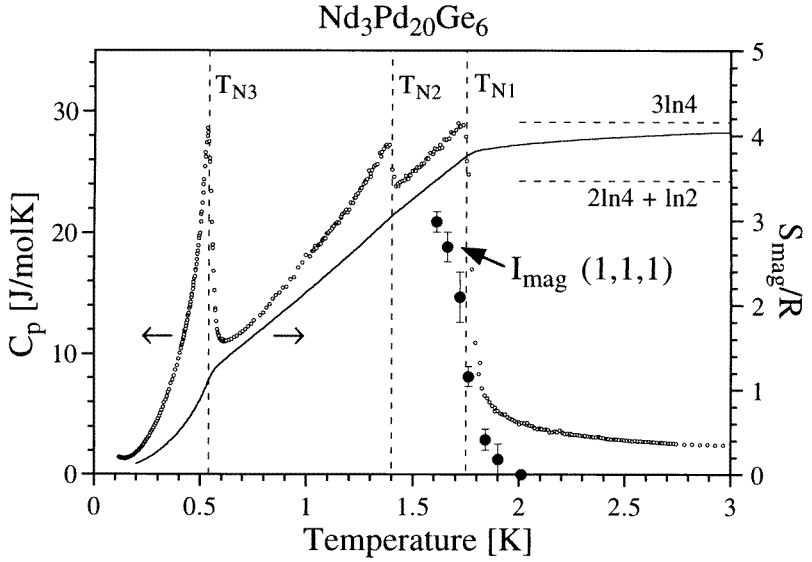

Figure 4. Temperature variation of the specific heat, C_p, the magnetic entropy, S_{mag}/R, and the magnetic neutron intensity $I_{mag}(1, 1, 1)$ for $Nd_3Pd_{20}Ge_6$. C_p and S_{mag}/R are plotted per formula unit $Nd_3Pd_{20}Ge_6$ and the neutron intensity in arbitrary units. The contribution to S_{mag}/R below 0.20 K was estimated as 0.126.

ions. Above T_{N1} the magnetic entropy S_{mag}/R, obtained by integrating C_p/T, saturates near the value 3ln4, implying quartets as CEF ground-states for all Nd atoms in $Nd_3Pd_{20}Ge_6$. (The possibility of a quartet as CEF ground-state at site 8c and a doublet at site 4a can be excluded because the corresponding magnetic entropy $S_{mag}/R = 3.47$ is clearly lower than the value $S_{mag}/R = 3.76$ released at $T_{N1} = 1.75$ K.)

Neutron diffraction measurements to determine the magnetic structure of $Nd_3Pd_{20}Ge_6$ between T_{N1} and T_{N2} were performed on D1A at 1.45 K (close to T_{N2}) and on DMC at

several temperatures between 1.6 and 3.0 K. Figure 5 compares the DMC diffraction patterns of $Nd_3Pd_{20}Ge_6$ measured in the paramagnetic state at 3.0 K (only nuclear contribution) and the difference pattern 1.6 K–3.0 K (only magnetic contribution). Magnetic Bragg intensity, which arises from scattering on ordered magnetic moments of Nd atoms, is observed for the reflections with odd indices ((1, 1, 1), (3, 1, 1) and (3, 3, 1) in figure 5) and *not* for those with even indices. With respect to the simple cubic lattice of the Nd2 atoms (nuclear Bragg peaks with even indices) the observed magnetic lines (reflections with odd indices) can all be indexed with an antiferromagnetic propagation vector $\boldsymbol{k} = [1, 1, 1]$. For the face-centred cubic lattice of the Nd1 atoms magnetic order implies the appearance of magnetic Bragg intensity at reflections with odd *and* even indices (in the case of a ferromagnetic structure) or at additional reflections which are forbidden by the crystal structure (in the case of an antiferromagnetic structure). Magnetic order of the Nd1 atoms is not observed in the diffraction pattern shown in figure 5. Thus, our neutron diffraction experiment reveals that the magnetic structure of $Nd_3Pd_{20}Ge_6$ between T_{N1} and T_{N2} corresponds to an antiferromagnetic stacking along the [1, 1, 1] direction of ferromagnetic (1, 1, 1) planes of ordered Nd2 moments (as illustrated in figure 2), and the Nd1 atoms are disordered. For such a magnetic structure, where the unit cells of the magnetic and crystallographic structures

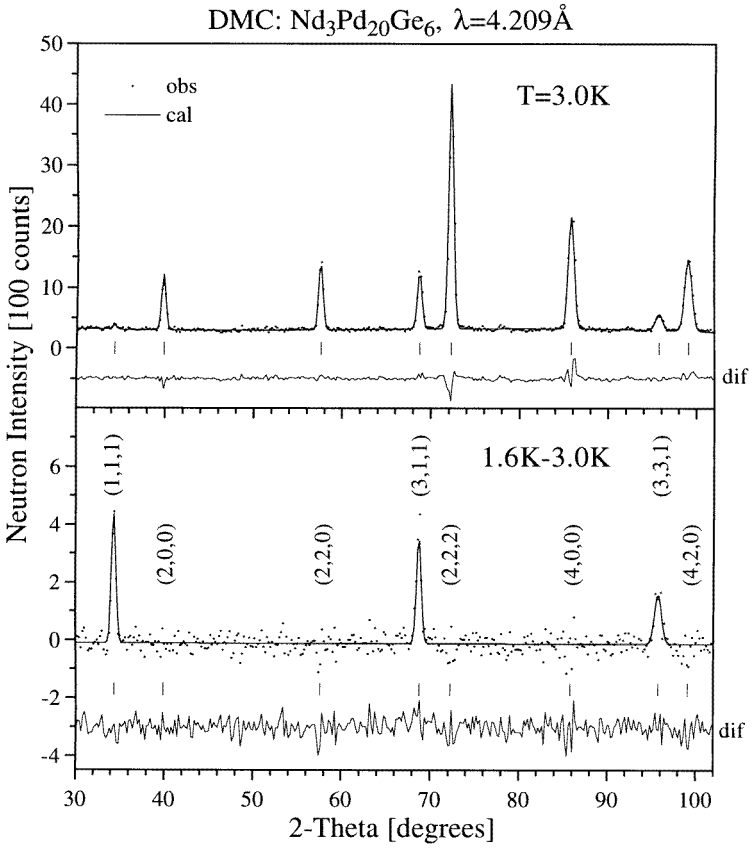

Figure 5. FullProf refinements of the crystal structure of $Nd_3Pd_{20}Ge_6$ at 3.0 K and of the antiferromagnetic structure of $Nd_3Pd_{20}Ge_6$ at 1.6 K (obtained from the difference pattern 1.6 K–3.0 K). Peak positions are indicated by vertical bars.

have the same size, the 'configurational symmetry' (defined in [8]) is cubic and the direction of the ordered Nd2 moments cannot be determined in a zero-field (single crystal or powder) neutron diffraction experiment [8]. In the case of equally populated magnetic domains the calculated magnetic neutron intensities become equal for any direction of the ordered Nd2 moments. Thus, our neutron diffraction experiments can only determine the amplitude of the ordered Nd2 moments and the kind of coupling between them. A one-parameter FullProf refinement of the DMC difference pattern 1.6 K–3.0 K (see lower frame of figure 5) yields an ordered magnetic Nd moment $\mu_2(\mathrm{Nd2}) = 1.4(1)\ \mu_B$ at 1.6 K ($\chi^2 = 1.00$). From the D1A pattern measured at 1.45 K the value $\mu_2(\mathrm{Nd2}) = 1.6(1)\ \mu_B$ was obtained by a simultaneous FullProf refinement of crystal and magnetic structures ($\chi^2 = 3.77$). For the strongest magnetic Bragg peak $(1, 1, 1)$ the temperature dependence of magnetic intensity $I_{mag}(1, 1, 1)$ is shown in figure 4. The ordered magnetic Nd2 moments appear in a second-order phase transition at T_{N1} and grow with decreasing temperature to $1.6(1)\ \mu_B$ at 1.45 K without reaching magnetic saturation. Because the interatomic Nd2–Nd2 distance (6.19 Å) is much shorter than the Nd1–Nd1 distance (8.76 Å) it is reasonable that magnetic order appears at higher temperature for the Nd2 atoms (at $T_{N1} = 1.75$ K) than for the Nd1 atoms (expected at $T_{N2} = 1.40$ K or at $T_{N3} = 0.54$ K).

3.3. Crystalline-electric-field excitations

The degeneracy of the J-multiplet of a magnetic ion embedded in a crystal lattice is partly removed by the CEF potential produced by the charge distribution of surrounding ions. In $Nd_3Pd_{20}Ge_6$ the magnetic Nd atoms occupy the two crystallographic sites 4a and 8c, which have both cubic point symmetry. For quantization along the fourfold $[0, 0, 1]$ direction the corresponding CEF Hamiltonian is given by

$$\begin{aligned} H_{CEF} &= B_4(O_4^0 + 5O_4^4) + B_6(O_6^0 - 21O_6^4) \\ &= W\left[\frac{x}{F(4)}(O_4^0 + 5O_4^4) + \frac{1-|x|}{F(6)}(O_6^0 - 21O_6^4)\right] \end{aligned} \tag{1}$$

where B_4 and B_6 are empirical CEF parameters which measure the strength of the fourth- and sixth-order terms of the electrostatic potential, respectively, and the O_n^m are operator equivalents built by spin operators [9]. The second line gives the equivalent Hamiltonian in terms of the CEF parameters W and x, introduced by Lea *et al* [10]. For Nd^{3+} the numerical factors are $F(4) = 60$ and $F(6) = 2520$. The tenfold degenerate ground-state J-multiplet $^4I_{9/2}$ of Nd^{3+} in $Nd_3Pd_{20}Ge_6$ decomposes into a doublet (Γ_6) and two quartets ($\Gamma_8^{(1)}$, $\Gamma_8^{(2)}$).

The interpretation of neutron spectroscopic data requires the identification of the observed CEF states with energy E_i by their correct representations Γ_i. This is usually achieved by comparing the observed intensities of the CEF transitions $|\Gamma_i\rangle \rightarrow |\Gamma_j\rangle$ with the differential neutron cross section, which for a system of N non-interacting ions is given in the dipole approximation by [11]

$$\begin{aligned} \frac{\mathrm{d}^2\sigma}{\mathrm{d}\Omega\,\mathrm{d}\omega} = \frac{N}{Z}\left(\frac{\gamma e^2}{m_e c^2}\right)\frac{k_1}{k_0}\exp[-2W(\boldsymbol{Q})]F^2(\boldsymbol{Q}) \\ \times \exp[-E_i/k_BT]|\langle\Gamma_i|J_\perp|\Gamma_j\rangle|^2\delta(E_i - E_j + \hbar\omega). \end{aligned} \tag{2}$$

Z is the partition function, k_0 and k_1 are the wave numbers of the incoming and scattered neutrons, respectively, $\exp[-2W]$ is the Debye–Waller factor, $F(\boldsymbol{Q})$ the magnetic form factor and $J_\perp$ the component of the total angular momentum operator perpendicular to the scattering vector $\boldsymbol{Q}$. The remaining symbols have their usual meaning. Intensities of CEF

transitions are decreasing with increasing scattering vector due to the form factor (in contrast to phonons whose intensities increase), and their temperature dependence is governed by Boltzman statistics. For Nd^{3+} with a cubic crystal field the transition probability matrix elements $(|\langle\Gamma_i|J_z|\Gamma_j\rangle|^2) = (|\langle\Gamma_i|J_\perp|\Gamma_j\rangle|^2)/2$ are plotted in figure 1 of [12] as a function of the CEF parameter x.

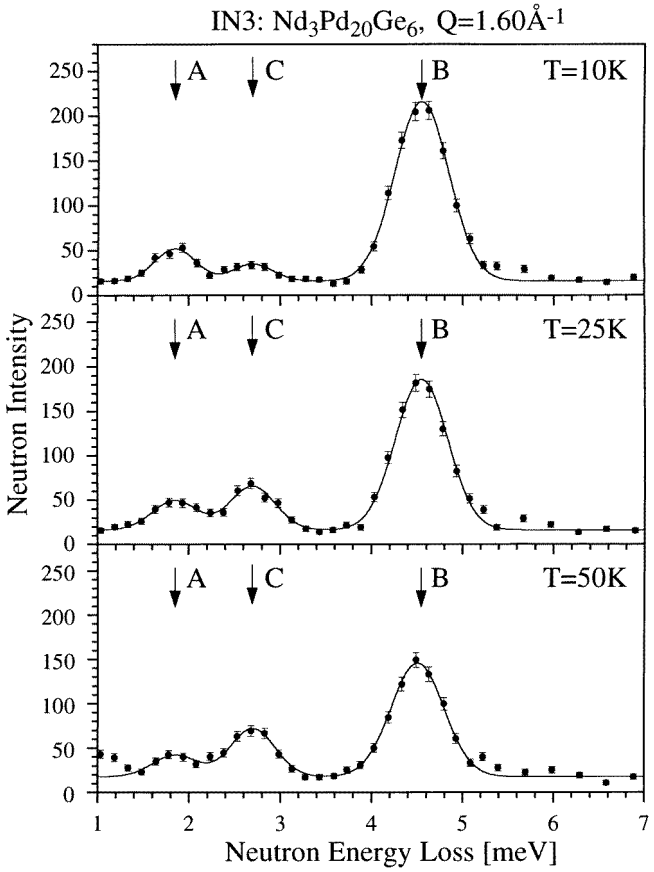

Figure 6. IN3 energy spectra at $T = 10$, 25 and 50 K of neutrons scattered from polycrystalline $Nd_3Pd_{20}Ge_6$ for $Q = 1.60$ Å^{-1} and fixed $E_f = 13.7$ meV. The curve corresponds to the fit of the total scattering and letters refer to CEF transitions of the diagram shown in figure 7.

The IN3 energy spectra of paramagnetic $Nd_3Pd_{20}Ge_6$, shown in figure 6, exhibit three inelastic lines, A at (1.85 ± 0.04) meV, B at (4.55 ± 0.02) meV and C at (2.70 ± 0.04) meV, which were all confirmed to be of magnetic origin by a measurement with a larger scattering vector $\boldsymbol{Q}$. Upon increasing the temperature from 10 K to 25 and 50 K the intensity is decreasing for the lines A and B and increasing for the excitation C. Thus, A and B can immediately be identified as ground-state CEF transitions, whereas C corresponds to a transition out of an excited CEF state. Keeping in mind that according to the magnetic entropy (see figure 4) the CEF ground-states of $Nd_3Pd_{20}Ge_6$ are quartets our IN3 experiment supports an interpretation of the lines A, B and C in figure 6 as the $\Gamma_8^{(1)} \rightarrow \Gamma_6$, $\Gamma_8^{(1)} \rightarrow \Gamma_8^{(2)}$ and $\Gamma_6 \rightarrow \Gamma_8^{(2)}$ transitions, respectively. The resulting CEF level diagram displayed in figure 7 gives rise to the values of the CEF parameters (B_4, B_6, W, x) and the calculated

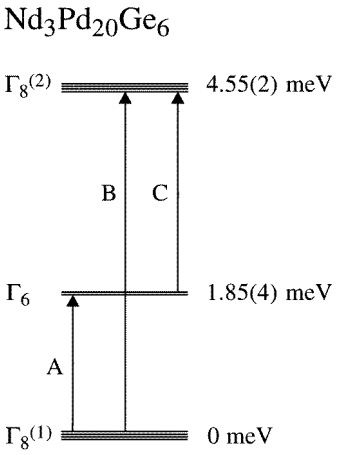

Figure 7. The CEF level diagram for $Nd_3Pd_{20}Ge_6$ derived from powder neutron scattering data. Letters refer to the CEF transitions shown in figure 6.

Table 2. CEF parameters (B_4, B_6, W, x) for $Nd_3Pd_{20}Ge_6$ and calculated energies (E_i), eigenfunctions (Γ_i) and transition probabilities ($|\langle\Gamma_i|J_\perp|\Gamma_j\rangle|^2$) obtained by a fit to powder neutron scattering data. Bold numbers correspond to CEF transitions with zero energy transfer.

CEF parameters:	$B_4 = (0.744 \pm 0.008) \times 10^{-3}$ meV		
	$B_6 = (0.130 \pm 0.004) \times 10^{-4}$ meV		
	$W = 0.773 \times 10^{-1}$ meV; $x = 0.578$		
Energies (meV):	$\Gamma_8^{(1)}(0) \rightarrow \Gamma_6(1.85) \rightarrow \Gamma_8^{(2)}(4.55)$		
Eigenfunctions:	$\Gamma_8^{(1)}$: $-0.0759\|\pm 9/2\rangle - 0.2002\|\pm 1/2\rangle + 0.9768\|\mp 7/2\rangle$		
	and $0.7802\|\pm 5/2\rangle - 0.6255\|\mp 3/2\rangle$		
	Γ_6: $0.6124\|\pm 9/2\rangle + 0.7638\|\pm 1/2\rangle + 0.2041\|\mp 7/2\rangle$		
	$\Gamma_8^{(2)}$: $0.7869\|\pm 9/2\rangle - 0.6137\|\pm 1/2\rangle - 0.0646\|\mp 7/2\rangle$		
	and $0.6255\|\pm 5/2\rangle + 0.7802\|\mp 3/2\rangle$		
Transition probabilities:	$\Gamma_8^{(1)}$	Γ_6	$\Gamma_8^{(2)}$
$\Gamma_8^{(1)}$	**46.89**	3.87	15.24
Γ_6		**13.44**	15.69
$\Gamma_8^{(2)}$			**35.07**

energies (E_i), eigenfunctions (Γ_i) and transition probabilities ($|\langle\Gamma_i|J_\perp|\Gamma_j\rangle|^2$) given in table 2. Calculated neutron intensities are in good agreement with the experiment: at 25 K the ratio Int(A)/Int(B) becomes 0.25 (calculated) and 0.2 ± 0.1 (observed, figure 6), whereas the ratio Int(A)/Int(C) results in 0.58 (calculated) and 0.7 ± 0.2 (observed, figure 6).

In $Nd_3Pd_{20}Ge_6$ the coordination polyhedra shown in figure 3 are different for Nd1 (12 Pd and 6 Ge nearest neighbours) and for Nd2 (16 Pd nearest neighbours). Therefore also the CEF parameters are expected to be different for the two Nd sites and CEF transitions of both CEF level diagrams should appear in the energy spectra. Nevertheless, our inelastic neutron scattering measurements did not show any evidence for an overlap of two independent CEF level schemes, i.e. all observed energies and intensities can be well explained with the single CEF level sequence shown in figure 7.

4. Summary and conclusions

For the new intermetallic compound $Nd_3Pd_{20}Ge_6$ we have presented an overview of the magnetic properties by measurements of the low-temperature specific heat (down to 0.12 K), neutron diffraction (down to 1.45 K) and inelastic neutron scattering (above 5 K). The refinement of the crystal structure at 10 K confirmed that $Nd_3Pd_{20}Ge_6$ is isostructural to $Ce_3Pd_{20}Ge_6$. $Nd_3Pd_{20}Ge_6$ crystallizes in the cubic space group $Fm\bar{3}m$ (No 225) and magnetic Nd atoms occupy the two different crystallographic sites 4a and 8c. Nd1 atoms on site 4a form a face-centred cubic lattice with a larger Nd1–Nd1 nearest-neighbour distance of 8.756(4) Å. Nd2 atoms on site 8c form a simple cubic lattice with a shorter Nd2–Nd2 nearest-neighbour distance of 6.192(3) Å. $Nd_3Pd_{20}Ge_6$ undergoes three successive magnetic phase transitions at $T_{N1} = 1.75$ K, $T_{N2} = 1.40$ K and $T_{N3} = 0.54$ K. Between T_{N1} and T_{N2} disordered Nd1 atoms coexist with antiferromagnetically ordered Nd2 atoms. The magnetic structure corresponds to an antiferromagnetic stacking along the [1, 1, 1] direction of ferromagnetic (1, 1, 1) planes of ordered Nd2 moments. The direction of the ordered Nd2 moments cannot be determined in a zero-field neutron diffraction experiment (because the configurational symmetry is cubic [8]) but a small crystal-electric-field anisotropy favours the [0, 0, 1] direction (expected moments of the CEF ground-state quartet $\Gamma_8^{(1)}$ are 2.40 μ_B, 2.35 μ_B and 2.32 μ_B along the [0, 0, 1], the [1, 1, 0] and the [1, 1, 1] direction, respectively). Further neutron diffraction experiments to determine the magnetic structures in $Nd_3Pd_{20}Ge_6$ below T_{N2} are planned in the near future. For paramagnetic $Nd_3Pd_{20}Ge_6$ we have established the CEF level scheme $\Gamma_8^{(1)} \rightarrow \Gamma_6(1.85\ \text{meV}) \rightarrow \Gamma_8^{(2)}(4.55\ \text{meV})$. Due to the large coordination number (18 for Nd1 and 16 for Nd2) the Nd ions in $Nd_3Pd_{20}Ge_6$ feel an electrostatic potential that is close to spherical and the resulting overall CEF splitting of 53 K is rather small compared with other Nd intermetallic compounds.

The CEF parameters determined for $Nd_3Pd_{20}Ge_6$ can be extrapolated to other trivalent rare-earth ions R in the same chemical structure $R_3Pd_{20}Ge_6$, since the CEF parameters then essentially scale with $\langle r^n \rangle$, the nth moment of the radial distribution of the 4f electrons, and with χ_n, the reduced matrix elements or Stevens factors, [13]:

$$B_n(\mathrm{R}) = B_n(\mathrm{Nd}) \frac{\langle r^n \rangle(\mathrm{R})}{\langle r^n \rangle(\mathrm{Nd})} \frac{\chi_n(\mathrm{R})}{\chi_n(\mathrm{Nd})}. \tag{3}$$

Such an extrapolation with no adjustable parameter yields the CEF level diagrams for $Pr_3Pd_{20}Ge_6$ and $Ce_3Pd_{20}Ge_6$ displayed in figure 8. As has been demonstrated for the

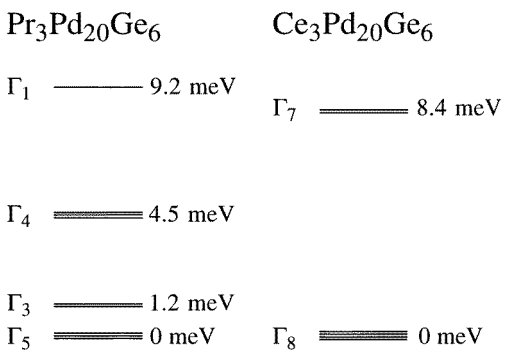

Figure 8. CEF level diagrams for $Pr_3Pd_{20}Ge_6$ and $Ce_3Pd_{20}Ge_6$ extrapolated from that of $Nd_3Pd_{20}Ge_6$.

rare-earth (R) compounds RPd_2Al_3 [14] and RPd_2Ga_3 [15], the extrapolation (3) is expected to give the correct qualitative energy distribution of CEF levels. For $Pr_3Pd_{20}Ge_6$ the validity of the CEF level scheme shown in figure 8 has been nicely confirmed by first inelastic neutron scattering data [16] which detected the CEF ground-state transitions $\Gamma_5 \rightarrow \Gamma_3 (\approx 0.4$ meV) and $\Gamma_5 \rightarrow \Gamma_4$ (4.0 meV) at slightly smaller energies than extrapolated. For $Pr_3Pd_{20}Ge_6$ with a CEF ground-state triplet Γ_5 we predict magnetic ordering at low temperature ($T < 1.5$ K). For $Ce_3Pd_{20}Ge_6$ the extrapolation tells us that the CEF ground-state is the quartet Γ_8, which has also been suggested by the magnetic entropy [1] and by the large Curie-type softening of the elastic constant $(C_{11} - C_{12})/2$ measured by ultrasonics [3]. Thus, both compounds $Ce_3Pd_{20}Ge_6$ and $Nd_3Pd_{20}Ge_6$ have a CEF ground-state quartet Γ_8, which possesses an electronic quadrupolar moment as well as a magnetic dipole moment. But in contrast to $Ce_3Pd_{20}Ge_6$, where quadrupolar ordering at $T_Q \approx 1.2$ K occurs at higher temperature than antiferromagnetic order at $T_N \approx 0.75$ K, in $Nd_3Pd_{20}Ge_6$ there is no quadrupolar ordering above T_{N1}.

Acknowledgments

We are indebted to Professor K A McEwen and Professor A Furrer for stimulating discussions. Financial support of the neutron scattering experiments by the Swiss National Science Foundation is gratefully acknowledged.

References

[1] Kitagawa J, Takeda N and Ishikawa M 1996 *Phys. Rev.* B **53** 5101
[2] Gribanov A V, Seropegin Y D and Bodak A I 1994 *J. Alloys Compounds* **204** L9
[3] Goto T and Suzuki O 1998 unpublished results
[4] Dönni A, Aso N and Endoh Y 1998 unpublished results
[5] Kitagawa J, Takeda N, Ishikawa M, Yoshida T, Ishiguro A, Kimura N and Komatsubara T 1998 *Phys. Rev.* B **57** 7450
[6] Rodriguez-Carvajal J 1993 *Physica* B **192** 55
[7] Sears V F 1992 *Neutron News* **3** 26
[8] Shirane G 1959 *Acta Crystallogr.* **12** 282
[9] Stevens K W H 1952 *Proc. Phys. Soc.* A **65** 209
[10] Lea K R, Leask M J M and Wolf W P 1962 *J. Phys. Chem. Solids* **23** 1381
[11] Trammel G T 1953 *Phys. Rev.* **92** 1387
[12] Birgeneau R J 1972 *J. Phys. Chem. Solids* **33** 59
[13] Fulde P 1979 *Handbook on the Physics and Chemistry of Rare Earths* ed K A Gschneidner and L Eyring Jr (Amsterdam: North-Holland) p 295
[14] Dönni A, Furrer A, Kitazawa H and Zolliker M 1997 *J. Phys.: Condens. Matter* **9** 5921
[15] Dönni A, Furrer A, Bauer E, Kitazawa H and Zolliker M 1997 *Z. Phys.* B **104** 403
[16] Keller L, Dönni A, Zolliker M and Komatsubara T 1999 *Physica* B to be published